Iranian Journal of Science
https://doi.org/10.1007/s40995-024-01665-1

RESEARCH PAPER

Multiple Bifurcations and Chaos Control in a Coupled Network of Discrete Fractional Order Predator–Prey System

Neriman Kartal[1]

Received: 20 March 2024 / Accepted: 7 June 2024

Abstract

Discrete-time dynamical system exhibits richer dynamical behaviors such as chaos rather than continuous-time dynamical systems. In order to describe chaos in two dimensional fractional order Lesli–Gower predator–prey systems, we need to transition from fractional continuous-time dynamical systems to the discrete-time version. One of the practical ways to achieve this transition is to use piecewise constant arguments in the model. After the discretization procedure based on the use of piecewise constant arguments in the interval $t \in [nh, (n+1)h)$, we obtain a new two dimensional system of difference equations. Necessary and sufficient conditions for the stability of the equilibrium points are given by using Schur–Cohn criterions. It is also investigated the existence of possible bifurcation types about the positive equilibrium point of the discrete system. Theoretical analysis shows that the system undergoes Neimark–Sacker and flip bifurcations with respect to parameter q. In addition, OGY feedback control method is implemented in order to control chaos in discrete model. Bifurcations in a coupled network of the discrete predator–prey system are also examined. Numerical simulations show that when the coupling strength parameter arrives the critical value, chaotic behavior is formed in the complex dynamical networks. All of the theoretical results dealing with the stability, bifurcation and transition chaos in the coupled network are stimulated by numerical simulations.

Keywords Complex network · Difference equation · Piecewise constant arguments · Bifurcation · Stability

MSC Classification 39A28 · 39A30 · 39A33 · 92B05 · 34K37

1 Introduction

Predator–prey interactions are one of the most fundamental areas in the population dynamics. The first and simplest mathematical model for this interaction was suggested by Lotka (1925) and Volterra (1926) independently in 1925 and 1926. Lotka-Volterra predator–prey models, which have successful applications in many fields such as biology (Hernández-Bermejo and Fairén 1997), chemistry (Sánchez-Pérez et al. 2020) and physics (Ma and Qian 2015), are still a hot topic that attracts the attention of researchers. Since the Lotka-Volterra predator–prey model neglects some biological facts, some modifications have been made by the researchers to improve realism. Leslie and Gower (1960) proposed a predator–prey model, so-called Leslie-Gower predator–prey model, where the carrying capacity of the predator's environment is a proportional to the number of prey. The new predator–prey system takes the following form:

$$\begin{cases} \dfrac{dx}{dt} = rx(t)(1 - x(t)) - x(t)y(t), \\ \dfrac{dy}{dt} = y(t)\left(p - \dfrac{qy(t)}{x(t)}\right), \end{cases} \tag{1}$$

where $x(t)$ and $y(t)$ represent the density of the prey and predator populations and the parameters r and p are growth rate of prey and predator population, respectively, also q denotes food quantity that prey provides and converted to predator birth. There are many studies in the literature dealing with the model (1) and its various modified versions can be found in Zhu et al. (2022), Gao and Yang (2022), Arancibia-Ibarra et al. (2022), Singh and Malik

✉ Neriman Kartal
nerimangok@nevsehir.edu.tr

[1] Department of Science and Mathematics Education, Faculty of Education, Nevsehir Haci Bektas Veli University, 50300 Nevsehir, Turkey

Published online: 02 July 2024

(2021), Vinoth et al. (2022), Khan et al. (2022), Li et al. (2020), Isık and Kangalgil (2022).

Recently, researchers have preferred to use fractional order differential equations instead of the ordinary counterpart in their mathematical model since these equations can reflect the whole period of the biological and physical process (Khan et al. 2021; Kumar et al. 2020a, b; Ghanbari and Kumar 2020; Kumar et al. 2021; Veeresha et al. 2020; Khajehnasiri et al. 2020; Rahmani Fazli et al. 2015; Khajehnasiri and Safavi 2021). There are a lot of definitions of fractional derivatives such as Caputo, Riemann Liouville, Atangana- Beleanu (ABC), Caputo–Fabrizio and Conformable. The fractional order version of the model (1) with Caputo sense is also studied in the literature as follows (Khoshsiar Ghaziani et al. 2016; Selvam and Jacob 2020; Rahmi et al. 2021; Li et al. 2018; Singh et al. 2019; Vahidi et al. 2021; Panigoro et al. 2021; Ghanbari 2021; Sekerci 2020; Kaviya and Muthukumar 2021):

$$\begin{cases} D^{\alpha}x(t) = rx(t)(1 - x(t)) - x(t)y(t), \\ D^{\alpha}y(t) = y(t)\left(p - \dfrac{qy(t)}{x(t)}\right), \end{cases} \tag{2}$$

where D^{α} represents fractional operator with Caputo sense. The ABC and Caputo-Fabrizio version of the model (2) are analyzed in the study (Panigoro et al. 2021) and (Sekerci 2020) respectively. On the other hand, in the study (Selvam and Jacob 2020; Singh et al. 2019) and (Vahidi et al. 2021) authors added piecewise constant arguments to Leslie-Gower predator–prey model and obtain the discrete version of the model (2).

Analysis of the dynamic characteristic of models such as stability, bifurcation, and chaos are tools that help us to understanding biological processes. Center manifold theory is one of the most important tools used to determine the stability of the discrete dynamical system as a result of bifurcation types such as flip and Neimark–Sacker bifurcations (Guckenheimer and Holmes 1983; Kangalgil 2019; Kangalgil and Isık 2020; Kaya et al. 2020). The chaotic structure can occurs as a result of these bifurcations and shows the complexity of the model.

Networks are a form of modeling that creates a topological structure by connecting construction whose elements interact with each other. Its history dates back to the Konigsberg 7 bridges problem in the 18th century and continue to exist as a branch of the graph theory until today. Although there are many different networks according to the shape of the connections, the most frequently used networks are globally coupled network, star network, nearest-neighbor coupled network, Erdos–Renyi network and scale free network. Networks are complex structures consisting of nodes and edges, and each node is represented by a nonlinear dynamical system in a complex network. Complex networks are one of the most interesting tools used to understand the origin and complexity of the dynamical system. The most important parameter that determines the dynamic behavior of complex networks is the coupling strength parameter. Increasing the heterogeneity of the network leads to a weakening of the coupling strength parameter, and as a result, the system may tend to exhibit chaotic behaviors. In the literature (Nepomuceno and Perc 2019; Li et al. 2004; Huang et al. 2019; Ahmed and Matouk 2020; Zhang et al. 2006; Wang et al. 2017), there are many works dealing with the stability and bifurcation analysis of the complex network. Nepomuceno and Perc (2019) investigated complex dynamics the Erdos Renyi network of the coupled logistic map. In this study, the authors demonstrated the transition from non-chaotic state to chaotic state on the dynamics of the network when the coupling strength parameter reaches a certain threshold value.

In ecology, it is very important to predict the behavior of populations through mathematical models. If the population is modeled through a continuous-time dynamical system, the behavior of the model is predictable. However, in discrete-time dynamical systems, the population exhibits unpredictable dynamical behavior such as chaotic oscillations under certain initial conditions. Experimental data have shown that many natural populations exhibit chaotic behavior (May 1976). Mathematically, we know that at least three-dimensional nonlinear differential equations are needed for continuous-time dynamical systems to see chaotic behavior. Therefore, the continuous-time dynamical system (2) is insufficient to describe the chaos that occurs in the predator–prey interactions. In order to obtain more realistic model, we will apply a discretization procedure to the model (2) and obtain a new discrete dynamical system. Hence discrete dynamical system includes the fractional order parameter as a new parameter. Although the existence and properties of chaos on complex continuous-time networks have been examined, there are not enough studies on its properties on fractional-order discrete-time complex networks. Analysis of dynamical behaviors such as chaos of the discrete-time prey-predator model on the complex networks will contribute to the literature.

The goal of the present study is to explore dynamical behavior of the discretized version of fractional order form of Leslie-Gower mathematical model (2) on both one single node and the coupled dynamical network. Basic definitions regarding fractional order derivative will be given in Sect. 2. In Sect. 3, a discretization method based on the using piecewise constant arguments is applied to the model (2) and we obtain system of difference equations. Stability analysis of the equilibrium points of the discrete system, Neimark Sacker and flip bifurcation analysis are given in

Sect. 4. Section 5 deals with the chaos control of the discrete model. In Sect. 6, the dynamic structure of the star network with $N = 10$ and $N = 100$ nodes are analyzed for the discrete time dynamical system. All theoretical results are supported by numerical simulations in Sect. 7. Finally, Sect. 8 supplies the conclusion.

2 Preliminaries of Fractional Calculus

In this section, let us briefly remember at some of the definitions in the field of fractional calculus.

Definition 1 (Kumar et al. 2020a) The Riemann–Liouville fractional derivative is given as follows:

$$ {}_{a}^{RL}D_t^q f(t) = \begin{cases} \dfrac{1}{\Gamma(n-q)} \dfrac{d^n}{dt^n} \displaystyle\int_a^t \dfrac{f(\tau)}{(t-\tau)^{(q-n+1)}}\, d\tau, & n-1<q<n, \\ \dfrac{d^n f(t)}{dt^n}, & q=n. \end{cases} \tag{3} $$

Definition 2 (Kumar et al. 2020a) The definition of Caputo fractional derivative is given as follows:

$$ {}_{a}^{C}D_t^q f(t) = \begin{cases} \dfrac{1}{\Gamma(n-q)} \displaystyle\int_0^t \dfrac{f^{(n)}(\tau)}{(t-\tau)^{(q-n+1)}}\, d\tau, & n-1<q<n, \\ \dfrac{d^n f(t)}{dt^n}, & q=n, \end{cases} \tag{4} $$

where n is the first integer which is not less than q. The symbol $\Gamma(.)$ is a gamma function characterize as:

$$ \Gamma(x) = \int_0^\infty \Omega^{x-1} e^{-\Omega}\, d\Omega, \quad (Re(x) > 0). \tag{5} $$

3 Discretization Process

In this section, we will discretize the model (2) based on use of piecewise constant arguments. Firstly, we consider the model (2) with piecewise constant arguments as follows.

$$ \begin{cases} D^\alpha x(t) = rx([\frac{t}{h}]h)(1 - x([\frac{t}{h}]h)) - x([\frac{t}{h}]h)y([\frac{t}{h}]h), \\ D^\alpha y(t) = y([\frac{t}{h}]h)\left(p - \dfrac{qy([\frac{t}{h}]h)}{x([\frac{t}{h}]h)}\right). \end{cases} \tag{6} $$

Let $t \in [0, h)$, then $\frac{t}{h} \in (0, 1)$. So we get

$$ \begin{cases} D^\alpha x(t) = rx_0(1 - x_0) - x_0 y_0, \\ D^\alpha y(t) = y_0\left(p - \dfrac{qy_0}{x_0}\right), \end{cases} \tag{7} $$

and the solution (6) is given by

$$ \begin{cases} x_1(t) = x_0 + I^\alpha(rx_0(1 - x_0) - x_0 y_0), \\ y_1(t) = y_0 + I^\alpha\left(y_0\left(p - \dfrac{qy_0}{x_0}\right)\right), \end{cases} \tag{8} $$

that is

$$ \begin{cases} x_1(t) = x_0 + \dfrac{t^\alpha}{\Gamma(\alpha+1)}(rx_0(1 - x_0) - x_0 y_0), \\ y_1(t) = y_0 + \dfrac{t^\alpha}{\Gamma(\alpha+1)}\left(y_0\left(p - \dfrac{qy_0}{x_0}\right)\right). \end{cases} \tag{9} $$

Let $t \in [h, 2h)$, then $\frac{t}{h} \in (1, 2)$. So we get

$$ \begin{cases} D^\alpha x(t) = rx_1(1 - x_1) - x_1 y_1, \\ D^\alpha y(t) = y_1\left(p - \dfrac{qy_1}{x_1}\right), \end{cases} \tag{10} $$

and the solution (6) is given by

$$ \begin{cases} x_2(t) = x_1(h) + I^\alpha(rx_1(1 - x_1) - x_1 y_1), \\ y_2(t) = y_1(h) + I^\alpha\left(y_1\left(p - \dfrac{qy_1}{x_1}\right)\right), \end{cases} \tag{11} $$

that is

$$ \begin{cases} x_2(t) = x_1(h) + \dfrac{(t-h)^\alpha}{\Gamma(\alpha+1)}(rx_1(h)(1 - x_1(h)) - x_1(h)y_1(h)), \\ y_2(t) = y_1(h) + \dfrac{(t-h)^\alpha}{\Gamma(\alpha+1)}\left(y_1(h)\left(p - \dfrac{qy_1(h)}{x_1(h)}\right)\right). \end{cases} \tag{12} $$

Repeating the process we can easily deduce that the solution of (6) is given by

$$ \begin{cases} x_{n+1}(t) = x_n(nh) + \dfrac{(t-nh)^\alpha}{\Gamma(\alpha+1)}(rx(nh)(1 - x(nh)) \\ \qquad -x(nh)y(nh)), \\ y_{n+1}(t) = y_n(nh) + \dfrac{(t-nh)^\alpha}{\Gamma(\alpha+1)}\left(y(nh)\left(p - \dfrac{qy(nh)}{x(nh)}\right)\right). \end{cases} \tag{13} $$

Let $t \to (n+1)h$, then we have

$$ \begin{cases} x_{n+1}((n+1)h) = x_n(nh) + \dfrac{h^\alpha}{\Gamma(\alpha+1)}(rx(nh)(1 - x(nh)) \\ \qquad -x(nh)y(nh)), \\ y_{n+1}((n+1)h) = y_n(nh) + \dfrac{h^\alpha}{\Gamma(\alpha+1)}\left(y(nh)\left(p - \dfrac{qy(nh)}{x(nh)}\right)\right), \end{cases} \tag{14} $$

that is

$$\begin{cases} x_{n+1} = x_n + \dfrac{h^\alpha}{\Gamma(\alpha+1)}(rx_n(1-x_n) - x_n y_n), \\ y_{n+1} = y_n + \dfrac{h^\alpha}{\Gamma(\alpha+1)}\left(y_n\left(p - \dfrac{qy_n}{x_n}\right)\right). \end{cases} \tag{15}$$

4 Stability and Bifurcation Analysis

4.1 Stability Analysis

The equilibrium points of system (15) are

$$E_1 = (1,0) \quad \text{and} \quad E_2 = \left(\frac{qr}{p+qr}, \frac{pr}{p+qr}\right). \tag{16}$$

Theorem 1 *The equilibrium point $E_1 = (1,0)$ is*

a) saddle point if $0 < r < \frac{2\Gamma(\alpha+1)}{h^\alpha}$,
b) source if $r > \frac{2\Gamma(\alpha+1)}{h^\alpha}$,
c) non-hyperbolic if $r = \frac{2\Gamma(\alpha+1)}{h^\alpha}$.

Proof The Jacobian matrix corresponding to the linearized system of the model (15) at the equilibrium point $E_1 = (1,0)$ can be calculated as follows.

$$J(E_1) = \begin{pmatrix} 1 - \dfrac{h^\alpha r}{\Gamma(\alpha+1)} & -\dfrac{h^\alpha}{\Gamma(\alpha+1)} \\ 0 & 1 + \dfrac{h^\alpha p}{\Gamma(\alpha+1)} \end{pmatrix}.$$

Moreover, the eigenvalues of this matrix are $\lambda_1 = 1 + \frac{h^\alpha p}{\Gamma(\alpha+1)}$ and $\lambda_2 = 1 - \frac{h^\alpha r}{\Gamma(\alpha+1)}$. It can be easily seen that $|\lambda_1| > 1$. In addition, if $0 < r < \frac{2\Gamma(\alpha+1)}{h^\alpha}$, then $|\lambda_1| < 1$. On the contrary, if $r > \frac{2\Gamma(\alpha+1)}{h^\alpha}$, then $|\lambda_2| > 1$. This completes the proof. □

Theorem 2 *Suppose that*

$$r > \frac{2\Gamma(\alpha+1)}{h^\alpha}, \tag{17}$$

and

$$0 < p < \frac{4(\Gamma(\alpha+1))^2}{rh^{2\alpha}}. \tag{18}$$

If

$$\frac{p^2(-rh^\alpha + \Gamma(\alpha+1))}{r(prh^\alpha - (p+r)\Gamma(\alpha+1))} < q < -\frac{p(ph^\alpha(rh^\alpha - 2\Gamma(\alpha+1)) + 4(\Gamma(\alpha+1))^2)}{r(ph^\alpha - 2\Gamma(\alpha+1))(rh^\alpha - 2\Gamma(\alpha+1))}, \tag{19}$$

then E_2 is local asymptotically stable.

Proof The calculations give the following Jacobian matrix at the equilibrium point E_2

$$J(E_2) = \begin{pmatrix} 1 - \dfrac{h^\alpha qr^2}{(p+qr)\Gamma(\alpha+1)} & -\dfrac{h^\alpha qr}{(p+qr)\Gamma(\alpha+1)} \\ \dfrac{h^\alpha p^2}{q\Gamma(\alpha+1)} & 1 - \dfrac{h^\alpha p}{\Gamma(\alpha+1)} \end{pmatrix},$$

which gives the characteristic equation

$$\lambda^2 + p_1\lambda + p_0 = 0, \tag{20}$$

where

$$p_1 = -2 + h^\alpha\left(\frac{p}{\Gamma(\alpha+1)} + \frac{qr^2}{(p+qr)\Gamma(\alpha+1)}\right), \tag{21}$$

and

$$p_0 = \frac{h^{2\alpha}pr(p+qr) - h^\alpha(p^2+pqr+qr^2)\Gamma(\alpha+1) + (p+qr)(\Gamma(\alpha+1))^2}{(p+qr)(\Gamma(\alpha+1))^2}. \tag{22}$$

To determine the stability conditions of the equilibrium point E_2, we can apply Jury conditions that are: a) $1 + p_1 + p_0 > 0$, b) $1 - p_1 + p_0 > 0$ and c) $1 - p_0 > 0$.

From the condition (a), we always hold

$$1 + p_1 + p_0 = \frac{h^{2\alpha}pr}{(\Gamma(\alpha+1))^2} > 0. \tag{23}$$

From (b) we have,

$$1 - p_1 + p_0 = 4 + \frac{h^\alpha\left(h^\alpha pr - \frac{2(p^2+pqr+qr^2)\Gamma(\alpha+1)}{p+qr}\right)}{(\Gamma(\alpha+1))^2}. \tag{24}$$

Considering the inequalities

$$0 < p < \frac{2\Gamma(\alpha+1)}{h^\alpha}, \tag{25}$$

and

$$0 < q < -\frac{p(ph^\alpha(rh^\alpha - 2\Gamma(\alpha+1)) + 4(\Gamma(\alpha+1))^2)}{r(ph^\alpha - 2\Gamma(\alpha+1))(rh^\alpha - 2\Gamma(\alpha+1))} \tag{26}$$

with the fact (17), then we have $1 - p_1 + p_0 > 0$. From (c), one can holds

$$1 - p_0 = \frac{h^\alpha\left(-h^\alpha pr + \frac{(p^2+pqr+qr^2)\Gamma(\alpha+1)}{p+qr}\right)}{(\Gamma(\alpha+1))^2}. \tag{27}$$

In addition, If

$$r > \frac{\Gamma(\alpha+1)}{h^\alpha}, \tag{28}$$

$$0<p<\frac{r\Gamma(\alpha+1)}{rh^{\alpha}-\Gamma(\alpha+1)}, \tag{29}$$

and

$$q>\frac{p^2(-rh^{\alpha}+\Gamma(\alpha+1))}{r(prh^{\alpha}-(p+r)\Gamma(\alpha+1))}, \tag{30}$$

then we have $1-p_0>0$. Consequently, considering the inequality (18), (25), (26), (28), (29) and (30) with together, we obtain the desired algebraic conditions. □

4.2 Bifurcation Analysis

Theorem 3 (*Wen 2005; Xin et al. 2010; Khan et al. 2022*) *Considering the following n-dimensional system with bifurcation parameter $q \in R$:*

$$X_{n+1}=f_q(X_n). \tag{31}$$

Suppose that characteristic polynomial of $J|_X$ about X of system (31) is

$$P(\lambda)=\lambda^n+p_1\lambda^{n-1}+p_2\lambda^{n-2}+\ldots+p_n. \tag{32}$$

Now considering the determinants $\Delta_0^{\pm}(q)=1$, $\Delta_1^{\pm}(q)$, \ldots,$\Delta_n^{\pm}(q)$, which can be defined as

$$\Delta_j^{\pm}(q)=\begin{vmatrix} 1 & p_1 & p_2 & \ldots & p_{j-1} \\ 0 & 1 & p_1 & \ldots & p_{j-2} \\ 0 & 0 & 1 & \ldots & p_{j-3} \\ \ldots & \ldots & \ldots & \ldots & \ldots \\ 0 & 0 & 0 & \ldots & 1 \end{vmatrix} \pm \begin{vmatrix} p_{n-j+1} & p_{n-j+2} & \ldots & p_{n-1} & p_n \\ p_{n-j+2} & p_{n-j+3} & \ldots & p_n & 0 \\ \ldots & \ldots & \ldots & \ldots & \ldots \\ p_{n-1} & p_n & \ldots & 0 & 0 \\ p_n & 0 & \ldots & 0 & 0 \end{vmatrix} \tag{33}$$

where $j=1,\ldots n$. Furthermore, Neimark–Sacker bifurcation occurs at critical value $q=q_0$ if following parametric condition hold:

NS1) Eigenvalue assignment: $P_{q_0}(1)>0$, $(-1)^nP_{q_0}(-1)>0$, $\Delta_{n-1}^{-}(q_0)=0$, $\Delta_{n-1}^{+}(q_0)>0$, $\Delta_j^{\pm}(q_0)>0$ where $j=n-3,n-5,\ldots 1$ (or 2), when n is even (or odd, respectively).

NS2) Transversality condition: $\frac{d}{dq}\Delta_{n-1}^{-}(q_0)\neq 0$.

NS3) Nonresonance condition: $\frac{cos(2\pi)}{l}\neq 1-(0.5)P_q(1)\frac{\Delta_{n-3}^{-}(q_0)}{\Delta_{n-2}^{+}(q_0)}$ or resonance condition $\frac{cos(2\pi)}{l}=1-(0.5)P_q(1)\frac{\Delta_{n-3}^{-}(q_0)}{\Delta_{n-2}^{+}(q_0)}$ where $l=3,4,\ldots$

Theorem 4 *Suppose that*

$$p<\frac{4(\Gamma(\alpha+1))^2}{rh^{2\alpha}}, \tag{34}$$

and

$$\frac{cos(2\pi)}{l}\neq 1-\frac{h^{2\alpha}pr}{2(\Gamma(\alpha+1))^2}. \tag{35}$$

If

$$q_0=\frac{p^2(-rh^{\alpha}+\Gamma(\alpha+1))}{r(prh^{\alpha}-(p+r)\Gamma(\alpha+1))}, \tag{36}$$

then Neimark–Sacker bifurcation emerges at the equilibrium point $E_2=(\frac{qr}{p+qr},\frac{pr}{p+qr})$ in the discrete dynamical system (15).

Proof By considering Theorem 3 for $n=2$, we have

$$P_q(1)=1+p_1+p_2>0, \tag{37}$$

$$(-1)^2P_q(-1)=1-p_1+p_2>0, \tag{38}$$

$$\Delta_1^{-}(q)=1-p_2=0, \tag{39}$$

$$\Delta_1^{+}(q)=1+p_2>0, \tag{40}$$

$$\frac{d}{dq}(\Delta_1^{-}(q))|_{q=q_0}=\frac{d}{dq}(1-p_2)|_{q=q_0}\neq 0, \tag{41}$$

and

$$\frac{cos(2\pi)}{l}\neq 1-(0.5)P_q(1)=1-\frac{1+p_1+p_2}{2}=\frac{1-p_1-p_2}{2}. \tag{42}$$

From (39), the critical Neimark–Sacker bifurcation point can be easily computed as in (36). Considering the inequalities (37) and (38) with the fact (34) one gets

$$P_{q_0}(1)=1+p_1+p_2=\frac{h^{2\alpha}pr}{(\Gamma(\alpha+1))^2}>0, \tag{43}$$

and

$$(-1)^2P_{q_0}(-1)=1-p_1+p_2=4-\frac{h^{2\alpha}pr}{(\Gamma(\alpha+1))^2}>0. \tag{44}$$

From (40), we have

$$\Delta_1^{+}(q)=1+p_2=2>0. \tag{45}$$

In addition, transversality condition (41) and non-resonance condition (42) give

$$\frac{d}{dq}(\Delta_1^-(q))|_{q=q_0} = \frac{h^\alpha(h^\alpha pr - (p+r)\Gamma(\alpha+1))^2}{p(\Gamma(\alpha+1))^3} \neq 0 \tag{46}$$

and

$$\frac{cos(2\pi)}{l} \neq 1 - \frac{h^{2\alpha}pr}{2(\Gamma(\alpha+1))^2}. \tag{47}$$

respectively. □

Theorem 5 (*Wen et al. 2008; Khan et al. 2022*) *Consider the system* (31) *with* $q \in R$ *is a bifurcation parameter. In addition, characteristic polynomial of* $J|_X$ *about X of system* (31) *is* (32). *Now considering the determinants* $\Delta_0^\pm(q) = 1, \Delta_1^\pm(q), \ldots, \Delta_n^\pm(q)$, *which are defined in* (33) *for* $j = 1, \ldots, n$. *Furthermore, flip bifurcation occurs at critical value* $q = q_0$ *if following parametric condition hold*:

FB1) Eigenvalue assignment: $P_{q_0}(1) > 0$, $P_{q_0}(-1) = 0$, $\Delta_{n-1}^\pm(q_0) > 0$, $\Delta_{n-1}^\pm(q_0) > 0$, $\Delta_j^\pm(q_0) > 0$ where $j = n-3, n-5, \ldots 1$ (or 2), when n is even (or odd, respectively).

FB2) Transversality condition: $\frac{\Sigma_{i=1}^n(-1)^{n-1}p_i'}{\Sigma_{i=1}^n(-1)^{n-i}(n-i+1)p_{i-1}} \neq 0$ where p_i' are the derivative with respect to q at $q = q_0$.

Theorem 6 *Suppose that*

$$p < \frac{4(\Gamma(\alpha+1))^2}{rh^{2\alpha}} \tag{48}$$

and

$$-\frac{h^{-\alpha}(h^\alpha p - 2\Gamma(\alpha+1))^2(h^\alpha r - 2\Gamma(\alpha+1))^2}{2p\Gamma(\alpha+1)(h^{2\alpha}pr - 3(\Gamma(\alpha+1))^2)} \neq 0. \tag{49}$$

If

$$q_0 = -\frac{p(h^{2\alpha}pr - 2h^\alpha p\Gamma(\alpha+1) + 4(\Gamma(\alpha+1))^2)}{r(h^\alpha p - 2\Gamma(\alpha+1))(h^\alpha r - 2\Gamma(\alpha+1))}, \tag{50}$$

then flip bifurcation emerges about the equilibrium point $E_2 = (\frac{qr}{p+qr}, \frac{pr}{p+qr})$ in the discrete dynamical system (15).

Proof By using Theorem 5 with $n = 2$, we have

$$P_q(1) = 1 + p_1 + p_2 > 0, \tag{51}$$

$$P_q(-1) = 1 - p_1 + p_2 = 0, \tag{52}$$

$$\Delta_1^-(q) = 1 - p_2 > 0, \tag{53}$$

$$\Delta_1^+(q) = 1 + p_2 > 0, \tag{54}$$

and

$$\frac{p_1' - p_2'}{3 - 2p_1} \neq 0. \tag{55}$$

From (52), the critical value of flip bifurcation point can be obtained as in (50). Considering the inequalities (51),(53) and (54) with the fact (48) one gets

$$P_{q_0}(1) = 1 + p_1 + p_2 = \frac{h^{2\alpha}pr}{(\Gamma(\alpha+1))^2} > 0, \tag{56}$$

$$\Delta_1^-(q_0) = 1 - p_2 = 2 - \frac{h^{2\alpha}pr}{2(\Gamma(\alpha+1))^2} > 0, \tag{57}$$

and

$$\Delta_1^+(q_0) = 1 + p_2 = \frac{h^{2\alpha}pr}{2(\Gamma(\alpha+1))^2} > 0. \tag{58}$$

From (55), one gets

$$\frac{p_1' - p_2'}{3 - 2p_1} = -\frac{h^{-\alpha}(h^\alpha p - 2\Gamma(\alpha+1))^2(h^\alpha r - 2\Gamma(\alpha+1))^2}{2p\Gamma(\alpha+1)(h^{2\alpha}pr - 3(\Gamma(\alpha+1))^2)} \neq 0. \tag{59}$$

□

5 Chaos Control

Although it is a real reality that populations exhibit unpredictable behavior in mathematical models, this is an undesirable result for scientists working in this field. In order to prevent the emergence of these unpredictable behaviors, that is chaos, mathematicians have resorted to some mathematical methods called chaos control strategies. In the literature, there are many chaos control methods such as OGY method, nonfeedback control and Pyragas method (Ott et al. 1990; Din 2017; Ramesh and Narayanan 1999; Pyragas 1992). To control the chaos in the system (15), we study feedback control strategy (OGY). Firstly, we reconsider (15) as the following form:

$$\begin{cases} x_{n+1} = x_n + \frac{h^\alpha}{\Gamma(\alpha+1)}(rx_n(1-x_n) - x_ny_n) = f(x_n, y_n, q), \\ y_{n+1} = y_n + \frac{h^\alpha}{\Gamma(\alpha+1)}\left(y_n\left(p - \frac{qy_n}{x_n}\right)\right) = g(x_n, y_n, q), \end{cases} \tag{60}$$

where q is taken as controlling parameter. In addition, q_0 is restricted to the line in some small interval $q \in (q_0 - \eta, q_0 + \eta)$ with $\eta > 0$, and q_0 is the nominal value belonging to chaotic region. Now, we can apply the stabilizing feedback control method in order to move the trajectory towards the desired orbit. Let $E_2 = (x^*, y^*) = (\frac{qr}{p+qr}, \frac{pr}{p+qr})$ be unstable equilibrium point of the discrete system in chaotic region formed by the emergence of flip bifurcation, then the system (60) can be approximated in the neighborhood of the unstable equilibrium point (x^*, y^*) by the following linear map:

$$\begin{bmatrix} x_{n+1} - x^* \\ y_{n+1} - y^* \end{bmatrix} \approx J(x^*, y^*, q_0) \begin{bmatrix} x_n - x^* \\ y_n - y^* \end{bmatrix} + B[q - q_0] \tag{61}$$

where

$$\begin{aligned} J(x^*, y^*, q_0) &= \begin{bmatrix} \dfrac{\partial f(x^*, y^*, q_0)}{\partial x} & \dfrac{\partial f(x^*, y^*, q_0)}{\partial y} \\ \dfrac{\partial g(x^*, y^*, q_0)}{\partial x} & \dfrac{\partial g(x^*, y^*, q_0)}{\partial y} \end{bmatrix} \\ &= \begin{bmatrix} 1 - \dfrac{h^\alpha q_0 r^2}{(p + q_0 r)\Gamma(\alpha + 1)} & -\dfrac{h^\alpha q_0 r}{(p + q_0 r)\Gamma(\alpha + 1)} \\ \dfrac{h^\alpha p^2}{q_0 \Gamma(\alpha + 1)} & 1 - \dfrac{h^\alpha p}{\Gamma(\alpha + 1)} \end{bmatrix}, \end{aligned}$$

and

$$B = \begin{bmatrix} \dfrac{\partial f(x^*, y^*, q_0)}{\partial q} \\ \dfrac{\partial g(x^*, y^*, q_0)}{\partial q} \end{bmatrix} = \begin{bmatrix} 0 \\ -\dfrac{h^\alpha p^2 r}{q_0 (p + q_0 r)\Gamma(\alpha + 1)} \end{bmatrix}. \tag{62}$$

Furthermore, the rank of the following matrix

$$\begin{aligned} C =& [B : JB] \\ =& \begin{bmatrix} 0 & \dfrac{h^{2\alpha} p^2 r^2}{(p + q_0 r)^2 (\Gamma(\alpha + 1))^2} \\ -\dfrac{h^\alpha p^2 r}{q_0 (p + q_0 r)\Gamma(\alpha + 1)} & \dfrac{h^\alpha p^2 r (h^\alpha p - \Gamma(\alpha + 1))}{q_0 (p + q_0 r)(\Gamma(\alpha + 1))^2} \end{bmatrix} \end{aligned} \tag{63}$$

is 2 that is system (60) is controllable with respect to parameter q.

Let

$$[q - q_0] = -K \begin{bmatrix} x_n - x^* \\ y_n - y^* \end{bmatrix}, \tag{64}$$

where $K = [\rho_1 \rho_2]$, then the system (61) can be re-written as follows:

$$\begin{bmatrix} x_{n+1} - x^* \\ y_{n+1} - y^* \end{bmatrix} \approx [J - BK] \begin{bmatrix} x_n - x^* \\ y_n - y^* \end{bmatrix}. \tag{65}$$

Now, the corresponding controlled system of (15) is given by

$$\begin{cases} x_{n+1} = x_n + \dfrac{h^\alpha}{\Gamma(\alpha + 1)} (r x_n (1 - x_n) - x_n y_n), \\ y_{n+1} = y_n + \dfrac{h^\alpha}{\Gamma(\alpha + 1)} (y_n (p - \dfrac{(q_0 - \rho_1 (x_n - x^*) - \rho_2 (y_n - y^*)) y_n}{x_n})). \end{cases} \tag{66}$$

The Jacobian matrix $J - BK$ of the controlled system (66) can be obtained as follows:

$$J - BK = \begin{bmatrix} 1 - \dfrac{h^\alpha q_0 r^2}{(p + q_0 r)\Gamma(\alpha + 1)} & -\dfrac{h^\alpha q_0 r}{(p + q_0 r)\Gamma(\alpha + 1)} \\ \dfrac{h^\alpha p^2}{q_0 \Gamma(\alpha + 1)} + \dfrac{h^\alpha p^2 r \rho_1}{q_0 (p + q_0 r)\Gamma(\alpha + 1)} & 1 - \dfrac{h^\alpha p}{\Gamma(\alpha + 1)} + \dfrac{h^\alpha p^2 r \rho_2}{q_0 (p + q_0 r)\Gamma(\alpha + 1)} \end{bmatrix}.$$

The equilibrium point (x^*, y^*) of the system (66) is locally asymptotically stable if and only if both eigenvalues of the characteristic equation $P(\lambda)$ of the jacobian matrix $J - BK$ lie inside the open unit disk where

$$P(\lambda)=\lambda^2+\lambda(-2+\frac{h^\alpha(q_0(p_2+pq_0r+q_0r^2)-p^2r\rho_2)}{q_0(p+q_0r)\Gamma(\alpha+1)})+\frac{q_0(p+q_0r)^2(\Gamma(\alpha+1))^2-h^\alpha(p+q_0r)\Gamma(\alpha+1)(q_0(p_2+pq_0r+q_0r^2)-p^2r\rho_2)}{q_0(p+q_0r)^2(\Gamma(\alpha+1))^2}+\frac{h^{2\alpha}pq_0r((p+q_0r)^2+pr(\rho_1-r\rho_2))}{q_0(p+q_0r)^2(\Gamma(\alpha+1))^2}.$$

Let λ_1 and λ_2 be the eigenvalues of the characteristic Eq. (67), then we get

$$\lambda_1+\lambda_2=2-\frac{h^\alpha(p^2+pq_0r+q_0r^2)}{(p+q_0r)\Gamma(\alpha+1)}+\frac{h^\alpha p^2r\rho_2}{q_0(p+q_0r)\Gamma(\alpha+1)}, \tag{67}$$

and

$$\lambda_1\lambda_2=1+\frac{h^\alpha(h^\alpha pr-\frac{(p^2+pq_0r+q_0r^2))\Gamma(\alpha+1)}{p+q_0r})}{(\Gamma(\alpha+1))^2}+\frac{h^{2\alpha}p^2r^2\rho_1}{(p+q_0r)^2(\Gamma(\alpha+1))^2}+\frac{h^\alpha p^2r(-h^\alpha q_0r^2+(p+q_0r)\Gamma(\alpha+1))\rho_2}{q_0(p+q_0r)^2(\Gamma(\alpha+1))^2}. \tag{68}$$

In order to obtain the lines of marginal stability, we take $\lambda_1=\pm1$ and $\lambda_1\lambda_2=1$. These restrictions make sure that the equilibrium point is locally asymptotically stable. Assuming that $\lambda_1\lambda_2=1$, then (68) implies that:

$$L_1:\frac{h^\alpha(h^\alpha pr(p+q_0r)-(p^2+pq_0r+q_0r^2)\Gamma(\alpha+1))}{(p+q_0r)(\Gamma(\alpha+1))^2}+\frac{h^{2\alpha}p^2r^2\rho_1}{(p+q_0r)^2(\Gamma(\alpha+1))^2}-\frac{h^\alpha p^2r(h^\alpha q_0r^2-(p+q_0r)\Gamma(\alpha+1))\rho_2}{q_0(p+q_0r)^2(\Gamma(\alpha+1))^2}=0.$$

From the equation $\lambda_1=1$, then (67) and (68) yield

$$L_2:\frac{h^\alpha pr(p+q_0r)}{\Gamma(\alpha+1)}+\frac{h^\alpha p^2r^2\rho_1}{(p+q_0r)\Gamma(\alpha+1)}-\frac{h^\alpha p^2r^3\rho_2}{(p+q_0r)\Gamma(\alpha+1)}=0.$$

Finally, taking $\lambda_1=-1$ and using the Eqs. (67) and (68) we hold

$$L_3:\frac{h^{2\alpha}pr(p+q_0r)-2h^\alpha(p^2+pq_0r+q_0r^2)\Gamma(\alpha+1)+4(p+q_0r)(\Gamma(\alpha+1))^2}{(p+q_0r)(\Gamma(\alpha+1))^2}+\frac{h^\alpha p^2r\rho_2}{q_0(p+q_0r)\Gamma(\alpha+1)}=-\frac{h^{2\alpha}p^2r^2\rho_1}{(p+q_0r)^2(\Gamma(\alpha+1))^2}+\frac{h^\alpha p^2r(h^\alpha q_0r^2-(p+q_0r)\Gamma(\alpha+1))\rho_2}{q_0(p+q_0r)^2(\Gamma(\alpha+1))^2}.$$

Then, stable eigenvalues lie within the triangular region in $\rho_1\rho_2$ plane bounded by the straight lines L_1, L_2, L_3 for particular parametric values.

6 Dynamical Analysis of the Model (15) on Star Network

Taking into account a dynamical network consisting of N linearly and diffusively coupled nodes, with each node describe a two-dimensional dynamical system defined by discrete system (15). Let's consider the model (15) as the following form:

$$\begin{cases} x(k+1) = x(k) + (rx(k)(1-x(k)) \\ \quad -x(k)y(k))\dfrac{h^\alpha}{\Gamma(\alpha+1)} = f(x(k), y(k)), \\ y(k+1) = y(k) + y(k)(p - \dfrac{qy(k)}{x(k)})\dfrac{h^\alpha}{\Gamma(\alpha+1)} = g(x(k), y(k)). \end{cases} \tag{69}$$

This dynamical network is defined by

$$\begin{cases} x_i(k+1) = f(x_i(k), y_i(k)) - c\sum_{j=1}^{N} a_{ij} f(x_j(k), y_j(k)), \\ y_i(k+1) = g(x_i(k), y_i(k)) - c\sum_{j=1}^{N} a_{ij} g(x_j(k), y_j(k)), \end{cases} \tag{70}$$

where i and j are the sequence number of the nodes in the

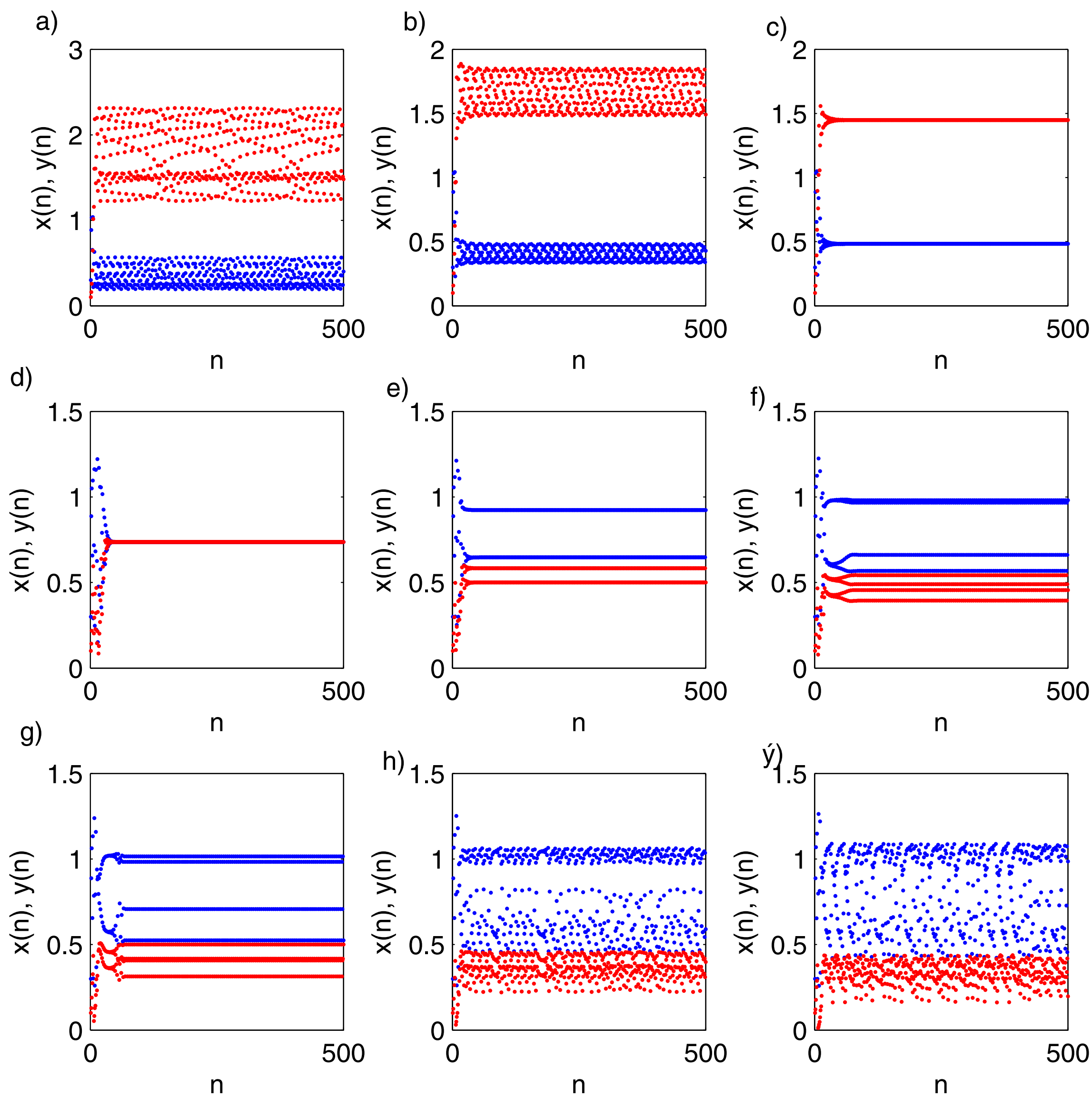

Fig. 1 Periodic orbits, stable and unstable equilibrium points with regard to parameter q: $q = 0.1$ **a**, $q = 0.141691$ **b**, $q = 0.2$ **c**, $q = 0.6$ **d**, $q = 0.814889$ **e**, $q = 0.9$ **f**, $q = 1$ **g**, $q = 1.1$ **h**, $q = 1.2$ **i**, where $\alpha = 0.95$, $p = 0.6$, $r = 2.8$, $h = 1$; $x(n)$ and $y(n)$ represent by blue and red curves respectively

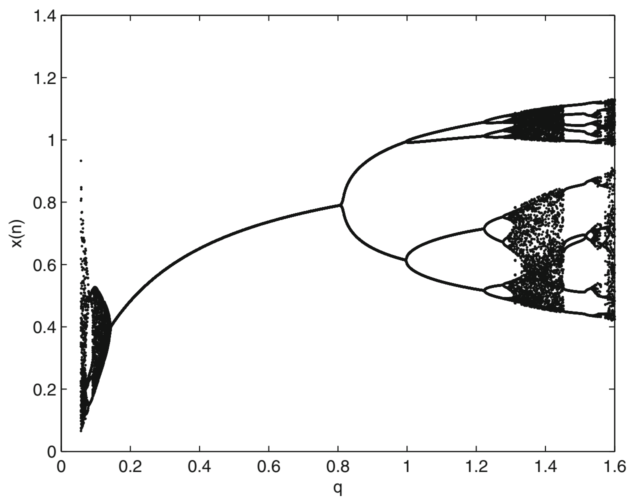

Fig. 2 Multiple bifurcation in the system (15) with regard to parameter q, where $\alpha = 0.95$, $p = 0.6$, $r = 2.8$, $h = 1$

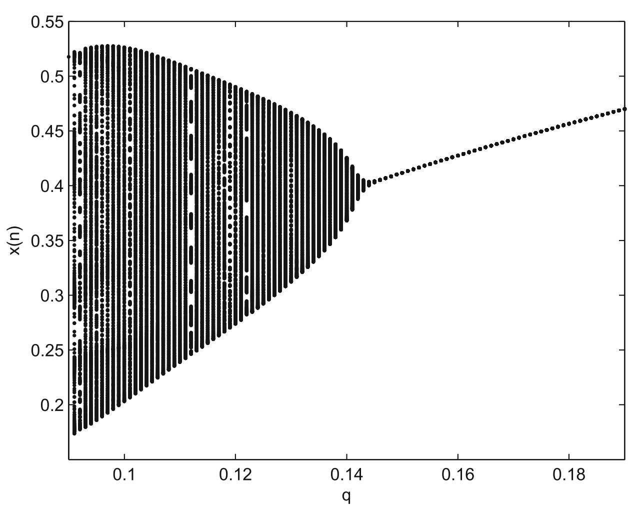

Fig. 3 Neimark–Sacker bifurcation in the system (15) with regard to parameter q, where $\alpha = 0.95$, $p = 0.6$, $r = 2.8$, $h = 1$

coupled dynamical network, c describes the coupling strength of the network. The coupling matrix $A \in R^{NxN}$ can be expressed by

$$A = \begin{pmatrix} d_{11} & a_{12} & a_{13} & \dots & a_{1N} \\ a_{12} & d_{22} & a_{23} & \dots & a_{2N} \\ a_{13} & a_{23} & d_{33} & \dots & a_{3N} \\ \vdots & \vdots & \vdots & \ddots & \dots \\ a_{1N} & a_{2N} & a_{3N} & \dots & d_{NN} \end{pmatrix}. \quad (71)$$

If there is a connection between node i and j, then $a_{ij} = 1$; otherwise, $a_{ij} = 0 (i \neq j)$. Let $a_{ii} = -d_i$, $i = 1, 2, \dots, N$, where d_i is the degree of node i and can be defined by the following equation:

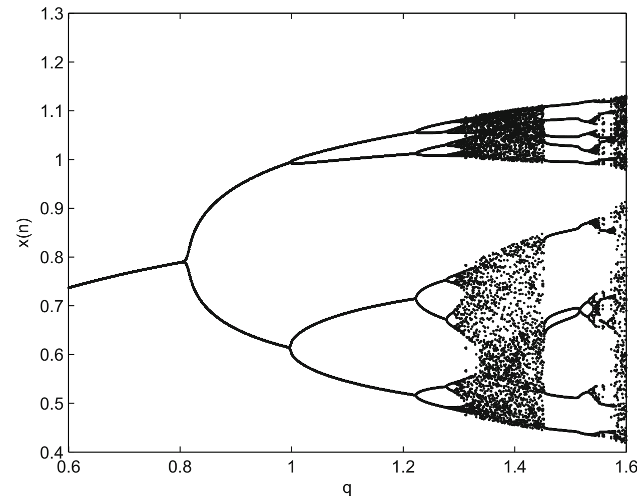

Fig. 4 Flip bifurcation in the system (15) with regard to parameter q, where $\alpha = 0.95$, $p = 0.6$, $r = 2.8$, $h = 1$

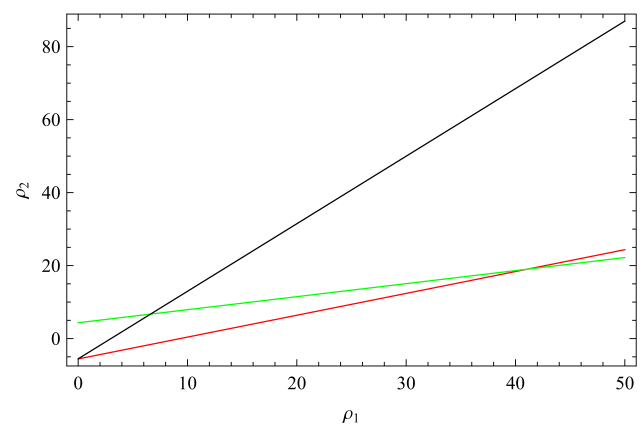

Fig. 5 Triangular stability region by L_1,L_2 and L_3 where $\alpha = 0.95$, $p = 0.6$, $r = 2.8$, $h = 1$, $q = 1.4$

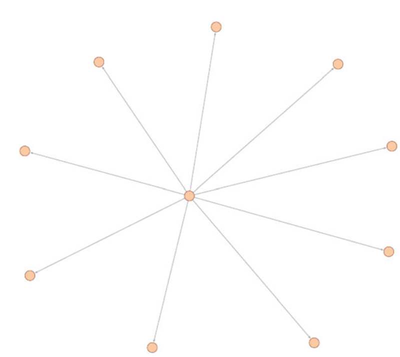

Fig. 6 Star network with $N = 10$

$$d_{ii} = -\sum_{j=1, j\neq i}^{N} a_{ij} = -\sum_{j=1, j\neq i}^{N} a_{ji}.$$

Now, system (70) can be rewritten as the following matrix form:

$$\begin{cases} X_{k+1} = (I - cA)f(X(k), Y(k)), \\ Y_{k+1} = (I - cA)g(X(k), Y(k)), \end{cases} \tag{72}$$

where $X_k = (x_1(k), x_2(k), \ldots, x_N(k))$, $Y_k = (y_1(k), y_2(k), \ldots, y_N(k))$ and $I \in R^{Nxn}$ is identity matrix.

7 Numerical Simulations

In this section, we use some numerical simulations to test the accuracy of the theoretical results. Let $\alpha = 0.95$, $p = 0.6$, $r = 2.8$ and $h = 1$. From the Theorem 2, we obtain the local asymptotically stable condition as $p < 1.37167$, $r > 1.95976$ and $0.141691 < q < 0.814889$. Figures 1 and 2 demonstrate that the equilibrium point of the discrete system is stable for some value of parameter q where it is in the range $0.141691 < q < 0.814889$, otherwise it is unstable. Figure 1a, c, d show stable equilibrium points; Fig. 1b and e demonstrate Neimark–Sacker and flip bifurcations respectively; Fig. 1f and g indicate periodic solutions; Fig. 1h and represent the chaotic behaviors. Figure 2 also shows multiple bifurcations such as Neimark–Sacker and flip bifurcation as the parameter q changes.

For the Neimark–Sacker bifurcation analysis, the parameter q is determined as a bifurcation parameter. From the condition of Theorem 4, we can select the model parameter as $\alpha = 0.95$, $p = 0.6$, $r = 2.8$ and $h = 1$ with the

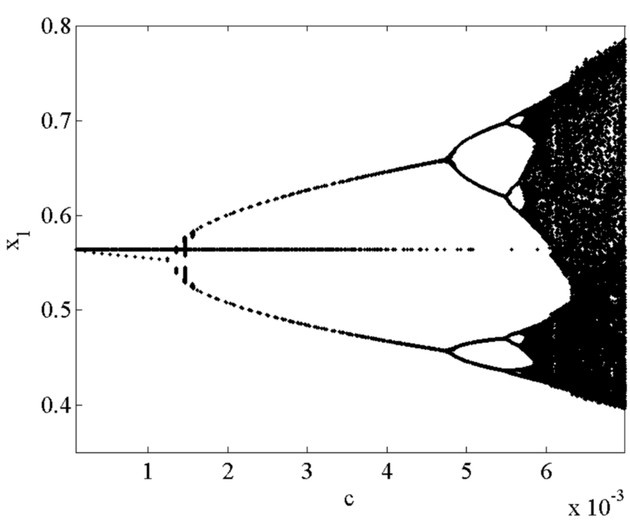

Fig. 7 Flip bifurcation in the star network with regard to parameter c, where $N = 10$ $\alpha = 0.95$, $p = 0.6$, $r = 2.8$, $h = 1$ and $q = 0.95$

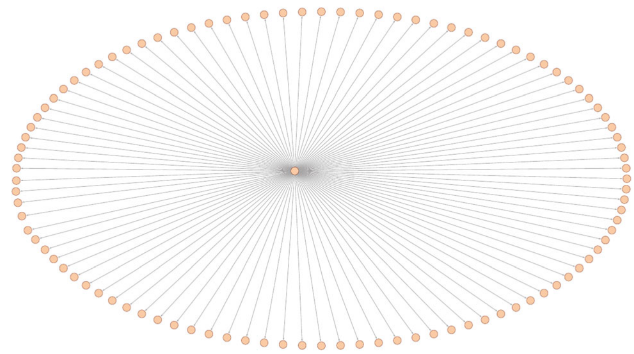

Fig. 8 Star network with $N = 100$

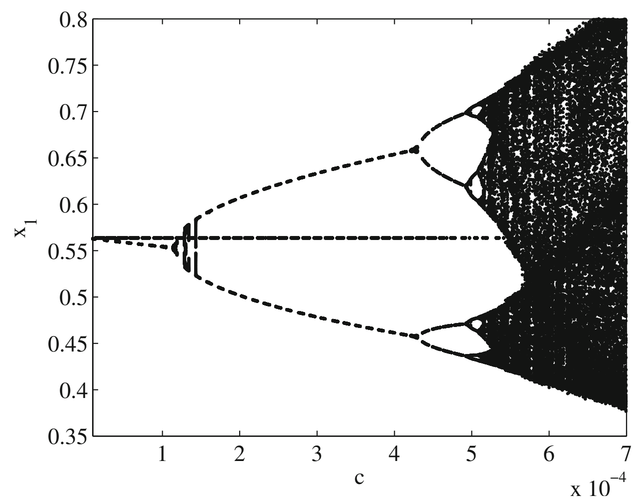

Fig. 9 Flip bifurcation in the star network with regard to parameter c, where $N = 10$ $\alpha = 0.95$, $p = 0.6$, $r = 2.8$, $h = 1$ and $q = 0.95$

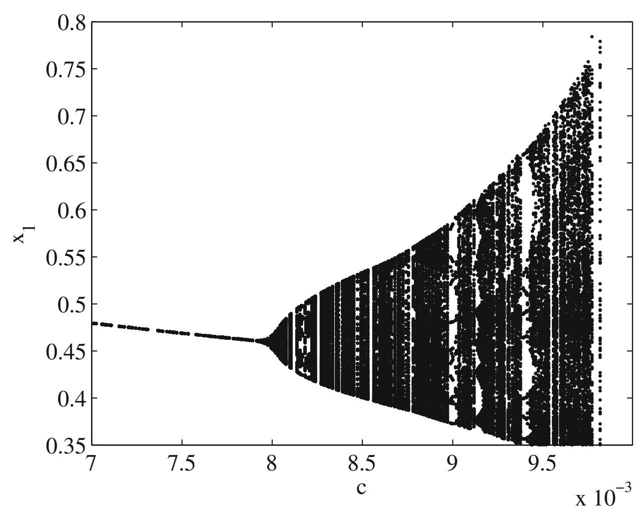

Fig. 10 Neimark–Sacker bifurcation in the star network with regard to parameter c, where $N = 100$ $\alpha = 0.95$, $p = 0.6$, $r = 2.8$, $h = 1$ and $q = 0.1$

fact that $p < 1.37167$. From the Eq. (36), we have the critical Neimark–Sacker bifurcation point as $q_0 = 0.141691$. Now, the characteristic equation becomes $\lambda^2 - 0.250303\lambda + 1 = 0$ that gives the complex eigenvalues $\lambda_{1,2} = 0.125151 \pm 0.992138i$. This eigenvalues satisfy the eigenvalue assignment condition $|\lambda_{1,2}| = 1$. In addition, from the Eq. (47) we have $l = \pm 4.34727$. Now all the conditions of Neimark–Sacker bifurcation are satisfied and this bifurcation is formed around the positive equilibrium point $E_2 = (0.398034, 1.68551)$ (Fig. 3).

As we consider the conditions of the flip bifurcation in Theorem 6 with the parameters $\alpha = 1$, $p = 0.95$, $r = 2.8$ and $h = 1$, we obtain the critical flip bifurcation point as $q_0 = 0.814889$ from the Eq. (50). Now, the characteristic equation becomes $\lambda^2 + 0.874849\lambda - 0.125151 = 0$ that gives the eigenvalues $\lambda_1 = -1$ and $\lambda_2 = 0.129151$. In addition, from the Eq. (59) we have $\frac{p_1^{'} - p_2^{'}}{3 - 2p_1} = 0.92473 \neq 0$. Now all conditions of flip bifurcation are satisfied and flip bifurcation takes place around the positive equilibrium point $E_2 = (0.791789, 0.582991)$ in the discrete dynamical system (15) (Fig. 4). Figure 3 and Fig. 4 are enlargement of Fig. 2 in two parts. (Fig. 5) gives the triangular stability region bounded by L_1, L_2 and L_3 for the controlled system (66). Staying within this triangular region, which permit us to control chaos, allows us to avoid unpredictable behavior.

The purpose here is to also investigate the complex dynamics of Leslie-Gower predator–prey system (15) into the coupled dynamical network. For this purpose we use the star network with $N = 10$ and $N = 100$ nodes. All simulations have used the same initial condition for all nodes, which are slightly different from the equilibrium point. Figure 6 shows the star network with $N = 10$ nodes. For this network with $N = 10$ nodes, the coupling matrix A can be computed from the Eq. (71) as follows:

$$A = \begin{pmatrix} -9 & 1 & 1 & 1 & 1 & 1 & 1 & 1 & 1 & 1 \\ 1 & -1 & 0 & 0 & 0 & 0 & 0 & 0 & 0 & 0 \\ 1 & 0 & -1 & 0 & 0 & 0 & 0 & 0 & 0 & 0 \\ 1 & 0 & 0 & -1 & 0 & 0 & 0 & 0 & 0 & 0 \\ 1 & 0 & 0 & 0 & -1 & 0 & 0 & 0 & 0 & 0 \\ 1 & 0 & 0 & 0 & 0 & -1 & 0 & 0 & 0 & 0 \\ 1 & 0 & 0 & 0 & 0 & 0 & -1 & 0 & 0 & 0 \\ 1 & 0 & 0 & 0 & 0 & 0 & 0 & -1 & 0 & 0 \\ 1 & 0 & 0 & 0 & 0 & 0 & 0 & 0 & -1 & 0 \\ 1 & 0 & 0 & 0 & 0 & 0 & 0 & 0 & 0 & -1 \end{pmatrix}$$

Now, let us consider the nodes in the networks with the highest degree that is x_1. Figure 7 depicts that when the coupling parameter c arrives the critical value where it is in the interval $c \in [1 \times 10^{-3}, 2 \times 10^{-3}]$, flip bifurcation emerges at the positive fixed point. We also investigate the dynamic structure of the complex network again by increasing the number of nodes where $N = 100$ (Fig. 8). Figure 9 demonstrates that the critical flip bifurcation point with respect to parameter c is the interval $c \in [1 \times 10^{-4}, 2 \times 10^{-4}]$.

The complex network with $N = 100$ nodes also exhibits Neimark–Sacker bifurcation about the positive equilibrium point with respect to parameter c where it is the interval $c \in [7.7 \times 10^{-3}, 8.2 \times 10^{-3}]$ (Fig. 10).

8 Conclusion

In this study, we examine dynamical behavior of the fractional order Leslie-Gower predator–prey model with piecewise constant arguments. The discretization method formed on the use piecewise constant arguments applies to predator–prey model and we obtain two dimensional discrete dynamical system (15). Some algebraic conditions to ensure the stability of the equilibrium points of the model are obtained by using Schur–Cohn criterion and these conditions are given in Theorem 1 and Theorem 2. Theorem 2 shows that the parameter q (food quantity) plays a key role on the dynamical behavior of the system (15). If the parameter q falls inside the range of inequality (19), then the positive equilibrium point of the system is local asymptotically stable. Figure 1 shows the both stable and unstable equilibrium points of the model depending on the change of the parameter q.

In Sect. 4, we investigate the existence of possible bifurcation types in the model and show that the model undergoes both Neimark–Sacker and flip bifurcations. Theorem 4 and Theorem 6 give us to necessary conditions of the existence these bifurcations respectively. The critical value of both Neimark–Sacker and flip bifurcations with respect to parameter q are given in Eq. (36) and (50) respectively. Figures 3 and 4 show that if the parameter q reaches these critical bifurcation point, then Neimark–Sacker and flip bifurcations occur around the positive equilibrium point.

In Sect. 4, we also deal with the discrete system (15) that represents a single node on the star network. System (70) can be used to represent a star network consisting of N nodes where interaction of each point is described by Leslie-Gower predator–prey model (15). Firstly, we investigate the dynamics of the star network with $N = 10$ nodes represented in Fig. 6. The most important parameter that determines the dynamics of such a complex network is the coupling strength parameter c. Figure 7 implies that if the parameter c falls in the interval $c \in [1 \times 10^{-3}, 2 \times 10^{-3}]$, flip bifurcation occurs around the positive equilibrium point. Secondly, we compose more complex network by increasing the numbers of nodes where $N = 100$ (Fig. 8). In such a network, flip bifurcation takes the form at a smaller value of c where it is in the range $c \in [1 \times 10^{-4}, 2 \times 10^{-4}]$. So, we can notice that as the number of node increases, bifurcation and chaotic dynamics appear at a lower coupling strength parameter c (Fig. 9). Figure 10 also demonstrates that complex network exhibits Neimark–Sacker bifurcation around the positive equilibrium point with respect to changing parameter c.

As can be seen in the theoretical and numerical simulations mentioned above, discrete-time dynamical system (15) exhibits rich dynamical behaviors such as multiple bifurcation and chaos which are not present in the continuous-time dynamical system (2). This illustrates the main reason why we focus on system (15) rather than system (2). On the other hand, the fact that the discrete dynamical system exhibits both flip and Neimark Sacker bifurcations according to changing parameter q (food quantity) that makes it even more interesting. Figure 2 clearly shows this rarely encountered situation. Although populations are in a steady state at the value of $q = 0.2$ where population sizes should not change as time goes on, decreasing or increasing the amount of food without foreseeing causes unpredictable behavior in the populations. A decrease in the amount of food quantity to 0.141691 causes a Neimark–Sacker bifurcation, and an increase to 0.814889 leads to flip bifurcation. After showing the existence of chaos, which are often encountered in population models, we present a strategy that can control this chaos. Figure 5 gives us the triangular region where we can control the chaos. Moreover, we show that the discrete-time dynamical system also exhibits the rich dynamical behaviors mentioned above on the complex networks.

Funding The authors declare that no funds, grants, or other support were received during the preparation of this manuscript.

Declarations

Conflict of interest The authors declare that they have no Conflict of interest.

References

Lotka AJ (1925) Elements of physical biology. Nature 116(2917):461–461. https://doi.org/10.1038/116461b0

Volterra V (1926) Fluctuations in the abundance of a species considered mathematically. Nature 118(2972):558–560. https://doi.org/10.1038/118558a0

Hernández-Bermejo B, Fairén V (1997) Lotka-volterra representation of general nonlinear systems. Math Biosci 140(1):1–32. https://doi.org/10.1016/s0025-5564(96)00131-9

Sánchez-Pérez JF, Conesa M, Alhama I, Cánovas M (2020) Study of lotka-volterra biological or chemical oscillator problem using the normalization technique: prediction of time and concentrations. Mathematics 8(8):1324. https://doi.org/10.3390/math8081324

Ma Y-A, Qian H (2015) A thermodynamic theory of ecology: Helmholtz theorem for lotka-volterra equation, extended conservation law, and stochastic predator-prey dynamics. Proc Royal Soc A: Math, Phys Eng Sci 471(2183):20150456. https://doi.org/10.1098/rspa.2015.0456

Leslie PH, Gower JC (1960) The properties of a stochastic model for the predator-prey type of interaction between two species. Biometrika 47(3/4):219. https://doi.org/10.2307/2333294

Zhu Z, Chen Y, Li Z, Chen F (2022) Stability and bifurcation in a leslie-gower predator-prey model with allee effect. Int J Bifurc Chaos. https://doi.org/10.1142/s0218127422500407

Gao Y, Yang F (2022) Persistence and extinction of a modified leslie-gower holling-type ii two-predator one-prey model with lévy jumps. J Biol Dyn 16(1):117–143. https://doi.org/10.1080/17513758.2022.2050313

Arancibia-Ibarra C, Flores JD, Heijster P (2022) Stability analysis of a modified leslie-gower predation model with weak allee effect in the prey. Front Appl Math Stat. https://doi.org/10.3389/fams.2021.731038

Singh A, Malik P (2021) Bifurcations in a modified leslie-gower predator-prey discrete model with michaelis-menten prey harvesting. J Appl Math Comput 67(1–2):143–174. https://doi.org/10.1007/s12190-020-01491-9

Vinoth S, Sivasamy R, Sathiyanathan K, Unyong B, Vadivel R, Gunasekaran N (2022) A novel discrete-time leslie-gower model with the impact of allee effect in predator population. Complexity 2022:1–21. https://doi.org/10.1155/2022/6931354

Khan MS, Abbas M, Bonyah E, Qi H (2022) Michaelis-menten-type prey harvesting in discrete modified leslie-gower predator-prey model. J Funct Spaces 2022:1–23. https://doi.org/10.1155/2022/9575638

Li Y, Zhang F, Zhuo X (2020) Flip bifurcation of a discrete predator-prey model with modified leslie-gower and holling-type iii schemes. Math Biosci Eng 17(3):2003–2015. https://doi.org/10.3934/mbe.2020106

Isık S, Kangalgil F (2022) On the analysis of stability, bifurcation, and chaos control of discrete-time predator-prey model with allee effect on predator. Hacettepe J Math Stat 51(2):404–420. https://doi.org/10.15672/hujms.728889

Khan MA, Ullah S, Kumar S (2021) A robust study on 2019-ncov outbreaks through non-singular derivative. Eur Phys J Plus. https://doi.org/10.1140/epjp/s13360-021-01159-8

Kumar S, Kumar A, Samet B, Dutta H (2020) A study on fractional host-parasitoid population dynamical model to describe insect species. Numer Methods Partial Differ Equ 37(2):1673–1692. https://doi.org/10.1002/num.22603

Kumar S, Chauhan RP, Momani S, Hadid S (2020) Numerical investigations on covid-19 model through singular and non-singular fractional operators. Numer Methods Partial Differ Equ. https://doi.org/10.1002/num.22707

Ghanbari B, Kumar S (2020) A study on fractional predator-prey-pathogen model with mittag-leffler kernel-based operators. Numer Methods Partial Differ Equ. https://doi.org/10.1002/num.22689

Kumar S, Kumar R, Momani S, Hadid S (2021) A study on fractional covid-19 disease model by using hermite wavelets. Math Methods Appl Sci 46(7):7671–7687. https://doi.org/10.1002/mma.7065

Veeresha P, Prakasha DG, Kumar S (2020) A fractional model for propagation of classical optical solitons by using nonsingular derivative. Math Methods Appl Sci. https://doi.org/10.1002/mma.6335

Khajehnasiri AA, Kermani MA, Ezzati R (2020) Chaos in a fractional-order financial system. Int J Math Opera Res 17(3):318. https://doi.org/10.1504/ijmor.2020.110028
Rahmani Fazli H, Hassani F, Ebadian A, Khajehnasiri AA (2015) National economies in state-space of fractional-order financial system. Afr Mat 27(3–4):529–540. https://doi.org/10.1007/s13370-015-0361-4
Khajehnasiri AA, Safavi M (2021) Solving fractional black-scholes equation by using boubaker functions. Math Methods Appl Sci 44(11):8505–8515. https://doi.org/10.1002/mma.7270
Khoshsiar Ghaziani R, Alidousti J, Eshkaftaki AB (2016) Stability and dynamics of a fractional order leslie-gower prey-predator model. Appl Math Model 40(3):2075–2086. https://doi.org/10.1016/j.apm.2015.09.014
Selvam AGM, Jacob SB (2020) Complex behavior in fractional - order leslie - gower prey - predator model with harvesting. AIP Conf. Proc. International conference on mathematical sciences and applications (ICMSA-2019) https://doi.org/10.1063/5.0014507
Rahmi E, Darti I, Suryanto A, Trisilowati H, Panigoro HS (2021) Stability analysis of a fractional-order leslie-gower model with allee effect in predator. J Phys: Conf Series 1821(1):012051. https://doi.org/10.1088/1742-6596/1821/1/012051
Li H-L, Muhammadhaji A, Zhang L, Teng Z (2018) Stability analysis of a fractional-order predator-prey model incorporating a constant prey refuge and feedback control. Adv Differ Equ. https://doi.org/10.1186/s13662-018-1776-7
Singh A, Elsadany AA, Elsonbaty A (2019) Complex dynamics of a discrete fractional-order leslie-gower predator-prey model. Math Methods Appl Sci 42(11):3992–4007. https://doi.org/10.1002/mma.5628
Vahidi A, Babolian E, Biranvand N (2021) Dynamical analysis stability and discretization of fractional-order predator-prey model with negative feedback on two species. Int J Nonlinear Anal Appl. https://doi.org/10.22075/ijnaa.2020.19764.2099
Panigoro HS, Suryanto A, Kusumawinahyu WM, Darti I (2021) Dynamics of an eco-epidemic predator-prey model involving fractional derivatives with power-law and mittag-leffler kernel. Symmetry 13(5):785. https://doi.org/10.3390/sym13050785
Ghanbari B (2021) A new model for investigating the transmission of infectious diseases in a prey-predator system using a non-singular fractional derivative. Math Methods Appl Sci 46(7):8106–8125. https://doi.org/10.1002/mma.7412
Sekerci Y (2020) Climate change effects on fractional order prey-predator model. Chaos, Solitons; Fractals 134:109690. https://doi.org/10.1016/j.chaos.2020.109690
Kaviya R, Muthukumar P (2021) Dynamical analysis and optimal harvesting of conformable fractional prey-predator system with predator immigration. Eur Phys J Plus. https://doi.org/10.1140/epjp/s13360-021-01559-w
Guckenheimer J, Holmes P (1983) Nonlinear oscillations, dynamical systems, and bifurcations of vector fields. Springer-Verlag, Berlin
Kangalgil F (2019) Neimark-sacker bifurcation and stability analysis of a discrete-time prey-predator model with allee effect in prey. Adv Differ Equ. https://doi.org/10.1186/s13662-019-2039-y
Kangalgil F, Isık S (2020) Controlling chaos and neimark-sacker bifurcation in a discrete-time predator-prey system. Hacettepe J Math Stat 49(5):1761–1776. https://doi.org/10.15672/hujms.531024
Kaya G, Kartal S, Gurcan F (2020) Dynamical analysis of a discrete conformable fractional order bacteria population model in a microcosm. Physica A 547:123864. https://doi.org/10.1016/j.physa.2019.123864
Nepomuceno EG, Perc M (2019) Computational chaos in complex networks. J Complex Netw. https://doi.org/10.1093/comnet/cnz015
Li X, Chen G, Ko K-T (2004) Transition to chaos in complex dynamical networks. Physica A 338(3–4):367–378. https://doi.org/10.1016/j.physa.2004.02.010
Huang T, Zhang H, Ma S, Pan G, Wang Z, Huang H (2019) Bifurcations, complex behaviors, and dynamic transition in a coupled network of discrete predator-prey system. Discret Dyn Nat Soc 2019:1–22. https://doi.org/10.1155/2019/2583730
Ahmed E, Matouk AE (2020) Complex dynamics of some models of antimicrobial resistance on complex networks. Math Methods Appl Sci 44(2):1896–1912. https://doi.org/10.1002/mma.6889
Zhang H-F, Wu R-X, Fu X-C (2006) The emergence of chaos in complex dynamical networks. Chaos, Solitons; Fractals 28(2):472–479. https://doi.org/10.1016/j.chaos.2005.07.001
Wang Z, Jiang G, Yu W, He W, Cao J, Xiao M (2017) Synchronization of coupled heterogeneous complex networks. J Franklin Inst 354(10):4102–4125. https://doi.org/10.1016/j.jfranklin.2017.03.006
May RM (1976) Simple mathematical models with very complicated dynamics. Nature 261(5560):459–467. https://doi.org/10.1038/261459a0
Wen G (2005) Criterion to identify hopf bifurcations in maps of arbitrary dimension. Phys Rev E 72(2):026201. https://doi.org/10.1103/physreve.72.026201
Xin B, Chen T, Ma J (2010) Neimark-sacker bifurcation in a discrete-time financial system. Discret Dyn Nat Soc 2010:1–12. https://doi.org/10.1155/2010/405639
Khan AQ, Qureshi SM, Alotaibi AM (2022) Bifurcation analysis of a three species discrete-time predator-prey model. Alex Eng J 61(10):7853–7875. https://doi.org/10.1016/j.aej.2021.12.068
Wen G, Chen S, Jin Q (2008) A new criterion of period-doubling bifurcation in maps and its application to an inertial impact shaker. J Sound Vib 311(1–2):212–223. https://doi.org/10.1016/j.jsv.2007.09.003
Ott E, Grebogi C, Yorke JA (1990) Controlling chaos. Phys Rev Lett 64(11):1196–1199. https://doi.org/10.1103/physrevlett.64.1196
Din Q (2017) Bifurcation analysis and chaos control in discrete-time glycolysis models. J Math Chem 56(3):904–931. https://doi.org/10.1007/s10910-017-0839-4
Ramesh M, Narayanan S (1999) Chaos control by nonfeedback methods in the presence of noise. Chaos, Solitons; Fractals 10(9):1473–1489. https://doi.org/10.1016/s0960-0779(98)00132-5
Pyragas K (1992) Continuous control of chaos by self-controlling feedback. Phys Lett A 170(6):421–428. https://doi.org/10.1016/0375-9601(92)90745-8